Title: Alumina/nano-graphite composite as a new nanosorbent for the selective adsorption, preconcentration, and determination of chromium in water samples by EDXRF

Author: Anna Baranik, Rafał Sitko, Anna Gagor, Beata Zawisza

Citation style: Baranik Anna, Sitko Rafał, Gagor Anna, Zawisza Beata. (2018). Alumina/nano-graphite composite as a new nanosorbent for the selective adsorption, preconcentration, and determination of chromium in water samples by EDXRF. "Analytical and Bioanalytical Chemistry" (Vol. 410, Iss. 29, s. 7793-7802), doi 10.1007/s00216-018-1397-8

RESEARCH PAPER

CrossMark

Alumina/nano-graphite composite as a new nanosorbent for the selective adsorption, preconcentration, and determination of chromium in water samples by EDXRF

Anna Baranik[1] · Rafal Sitko[1] · Anna Gagor[2] · Beata Zawisza[1]

Abstract

Obtaining new nanocomposites with sorption properties towards chromium is highly important not only from the environmental point of view but also for developing eco-friendly methods of chromium determination. The potential use of aluminum oxide-coated nano-graphite (Al_2O_3/nano-G) as a new nanosorbent in ultrasound-assisted dispersive micro-solid-phase extraction (DMSPE) for rapid speciation of trace chromium(III) and chromium(VI) ions in natural water was evaluated. In the developed method, the crucial issue is the new nanocomposite synthesized by coating alumina on a nano-graphite surface with sorption properties. Structural researches of the nanocomposite were carried out by scanning electron microscopy (SEM), powder X-ray diffraction (XRD), and Raman spectroscopy. Maximum adsorption capacity of Al_2O_3/nano-G towards Cr(III) was 32.8 mg g^{-1}. The influence of the method's factors like pH, sample volumes, contact time, coexisting ions, and humic acid on the recovery of chromium was examined. The nanocomposites have been found to be stable and effective as a sorbent in water with high concentrations of selected cations and anions present in water as well as in water of various pH. Al_2O_3/nano-G is selective for Cr(III) in presence of Cr(VI). Cr(III) was determined by the developed method, total Cr after reduction of Cr(VI) to Cr(III), and Cr(VI) was calculated as the difference between total Cr and Cr(III). After sorption, the nanocomposite with chromium was collected on 5-mm diameter filters and analyzed by energy-dispersive X-ray fluorescence spectrometry (EDXRF) to determine the chromium concentration. The method was characterized by correlation coefficient 0.999, limit of detection (LOD) 0.04 ng mL^{-1}, and relative standard deviation (RSD) 3.5%. Al_2O_3/nano-G combined with proposed DMSPE/EDXRF was verified by analysis of certificate reference material of natural water (NIST 1640a).

Keywords Preconcentration · Speciation · Trace analysis · Nanosorbent · Environmental samples · Sorption

Introduction

The interest in chromium speciation originates from widespread use of this metal in various industries such as chemical, metallurgical, and refractories. Thus, large quantities of chromium compounds are discharged in solid, liquid, and gaseous wastes into the environment and can have potentially adverse biological and ecological effects. The two widespread oxidation states of Cr are present in the environment, i.e., Cr(III) and Cr(VI). They are drastically different in chemical and biochemical reactivity and physicochemical properties [1]. Cr(III) is considered to be a trace element essential for the proper functioning living organisms, but in a significant concentration can cause adverse effects because of its high capability to coordinate various organic compounds, whereas Cr(VI) is considered exerting toxic effects on biological systems. It was found that exposure to hexavalent Cr compounds can lead to a variety of clinical problems [2]. Thus, a detailed knowledge of each species rather than the total chromium level is required to properly evaluate its toxicological effects, and distribution in the environment. The concentration of chromium in environment is controlled and observed by the World Health Organization (WHO) [3] and the Environmental Protection Agency (EPA) [4]. WHO and EPA have

✉ Beata Zawisza
beata.zawisza@us.edu.pl

[1] Institute of Chemistry, University of Silesia, Szkolna 9, 40-006 Katowice, Poland

[2] Institute of Low Temperature and Structure Research, Polish Academy of Sciences, P.O. Box 1410, 50-950 Wrocław, Poland

Springer

established an upper concentration limit for chromium in drinking water, which equals 50 ng mL^{-1} and 100 ng mL^{-1}, respectively.

The literature proposes a lot of methods to oxidation and/or reduction of chromium before the removal/separation. The Cr(III) ions can be oxidized by potassium permanganate solution ($KMnO_4$) [5, 6], hydrogen peroxide (H_2O_2) [7, 8], or potassium peroxodisulfate ($K_2S_2O_8$) in acid solution [9]. Many methods allowing reducing Cr(VI) ions are also shown in the literature. The concentrated sulfuric acid (H_2SO_4) with ethanol (C_2H_5OH) [10, 11], hydroxylamine hydrochloride ($NH_2OH \cdot HCl$) solution [12–14], or hydrochloric acid (HCl) solution with C_2H_5OH [15] has played a good role in complete reduction of Cr(VI).

For determination of trace amounts of chromium in different materials, oxidized multiwalled carbon nanotubes (MWCNTs) [14], MWCNTs modified with the anionic exchanger tricaprylmethylammonium chloride (Aliquat 336) [16], graphene oxide (GO) [11], graphene oxide decorated with triethylenetetramine-modified magnetite (mf-GO) [17], and graphene (G) [18] were applied. The trace amount of chromium ions was preconcentrated using solid-phase extraction (SPE) [18] and dispersive magnetic SPE [17] combined with flame atomic absorption spectrometry (FAAS), dispersive micro-solid-phase extraction (DMSPE) combined with total reflection X-ray fluorescence (TXRF) [16], and energy-dispersive X-ray fluorescence spectrometry (EDXRF) [11]. Several carbon sorbents have also high affinity for both chromium and other heavy metals. Oxidized MWCNTs [19], 3-(2-aminoethylamino) propyltrimethoxysilane (AAPTS) functionalized MWCNTs [6], Schiff base-chitosan-grafted MWCNTs (S-CS-MWCNTs) [20], nano-graphite [21], GO nanosheets [22], and GO connected with 2-(5-bromo-2-pyridylazo)-5-diethylaminophenol (5-Br-PADAP) [23] have found analytical application in the sorption and determination not only of Cr(III) and Cr(VI) but also of Mn(II), Fe(III), Co(II), Ni(II), Cu(II) Pb(II), As(V), Se(VI), and V(V). Our previous studies have shown that alumina supported on graphene oxide (Al_2O_3/GO) can be successfully used for preconcentration of As(V) and Cr(III) [24].

In this work, the alumina was supported on nano-graphite to obtain Al_2O_3/nano-G composite suitable for selective sorption of chromium in both batch and under flow conditions. Thanks to microscopy and spectroscopy researches, Al_2O_3/nano-G composite structure was confirmed and characterized. The maximum adsorption capacity of the new nanosorbent was evaluated by Langmuir isotherm model. Al_2O_3/nano-G composite was applied in DMSPE combined with EDXRF. The advantage of this methodology over ICP-OES, ICP-MS, and FAAS is the possibility of direct determination of analyte onto sorbent without elution. Thus, errors connected with contamination of sample or losses of analyte are eliminated and time of sample preparation is shortened. The preconcentration

of Cr(III) by Al_2O_3/nano-G can be performed within 5 min. The obtained samples are durable; thus, they can be stored and analyzed many times as well as can be used in further research. Analytes can be also determined after elution from nanocomposite, using alternative techniques. Application of Al_2O_3/nano-G in DMSPE/EDXRF method allows for direct determination of trace amounts of Cr(III) in environment water samples. The developed methodology is environmentally friendly and non-time-consuming.
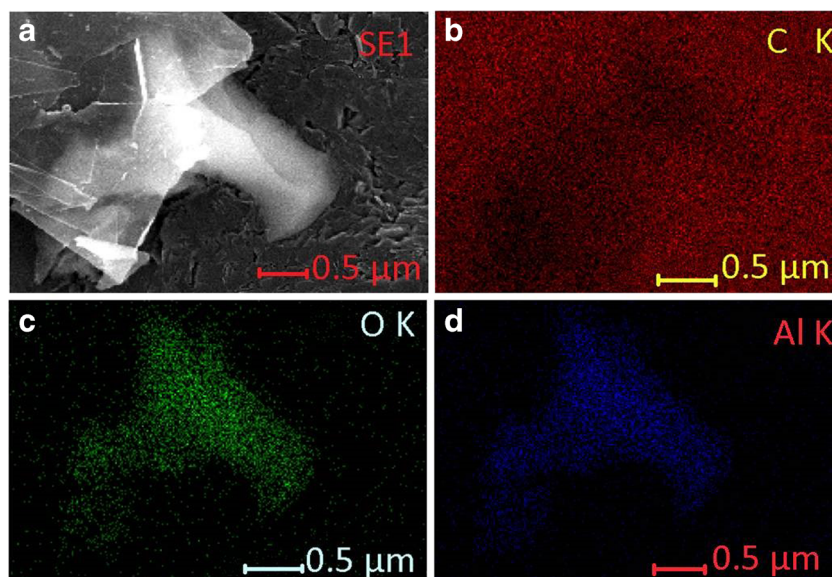
Materials and methods

Materials

Chromium stock solution 1 mg mL^{-1} of Cr(III) and Cr(VI) was purchased from Merck (Darmstadt, Germany); humic acid was purchased from Sigma-Aldrich (Steinheim, Germany); graphene nanopowder 8 nm (purity 99.99% and the flakes size 8 nm) was purchased from graphene supermarket (New York, USA); nitric acid (65%, Suprapur®), ammonium hydroxide solution (25%, Suprapur®), ethanol (96% p.a.), sulfuric acid (96% p.a.), Triton X-100 (p.a.), chromium(III) nitrate nanohydrate (p.a.), sodium nitrate (p.a.), potassium nitrate (p.a.), calcium nitrate tetrahydrate (p.a.), magnesium nitrate hexahydrate (p.a.), iron(III) nitrate nanohydrate (p.a.), aluminum nitrate nanohydrate (p.a.), buffer solution (pH 4.00 ± 0.05 and pH 7.00 ± 0.05), and the Munktell membrane filters of thickness 176 μm (no. 391) were purchased from Avantor Performance Materials Poland S.A. (Gliwice, Poland). Standard solutions were diluted with high-purity water obtained from Milli-Q system (Millipore, Molsheim, France). Certified Reference Material (natural water 1640a) was purchased from National Institute of Standards and Technology (Gaithersburg, USA).

Apparatus

The microstructural observation of the Al_2O_3/nano-G was on a JEOL-7600F scanning electron microscope (SEM) (Oregon, USA) equipped with the Oxford X-ray energy-dispersive spectrometer (EDS). Powder X-ray diffraction data (XRD) (PANalytical, Almelo, The Netherlands) were collected on X'Pert PRO X-ray diffractometer with PIXcel ultrafast line detector and Soller slits for Cu K$_\alpha$ radiation. The measurements were done in Bragg-Brentano geometry.

The Raman spectra (Renishaw, New Mills, Wotton-under-Edge Gloucestershire, UK) were measured at room temperature using RenishawInVia Raman spectrometer equipped with confocal DM 2500 Leica optical microscope, a thermoelectrically cooled Ren Cam CCD detector and a diode laser operating at 830 nm.

Fig. 1 SEM images of synthesized Al₂O₃/nano-G (**a**) and maps of the correlation between distribution of carbon (**b**), oxygen (**c**), and aluminum (**d**) on the Al₂O₃/nano-G surface

The EDXRF spectra were measured by energy-dispersive X-ray fluorescence spectrometer Epsilon 3 (PANalytical, Almelo, The Netherlands) with the Rh target X-ray tube with 50-μm Be window and max. power of 9 W. The spectrometer is equipped with thermoelectrically cooled silicon drift detector (SDD) with 8-μm Be window and resolution of 135 eV at 5.9 keV. The spectrometer is equipped with spinner and five primary filters that can be selected to improve measuring conditions for determined elements. The measurement conditions are 20 kV, 450 μA, Al filter of 200-μm thickness, air atmosphere, and 300 s of measure time. The samples were packed in mylar foil of 6-μm thickness.
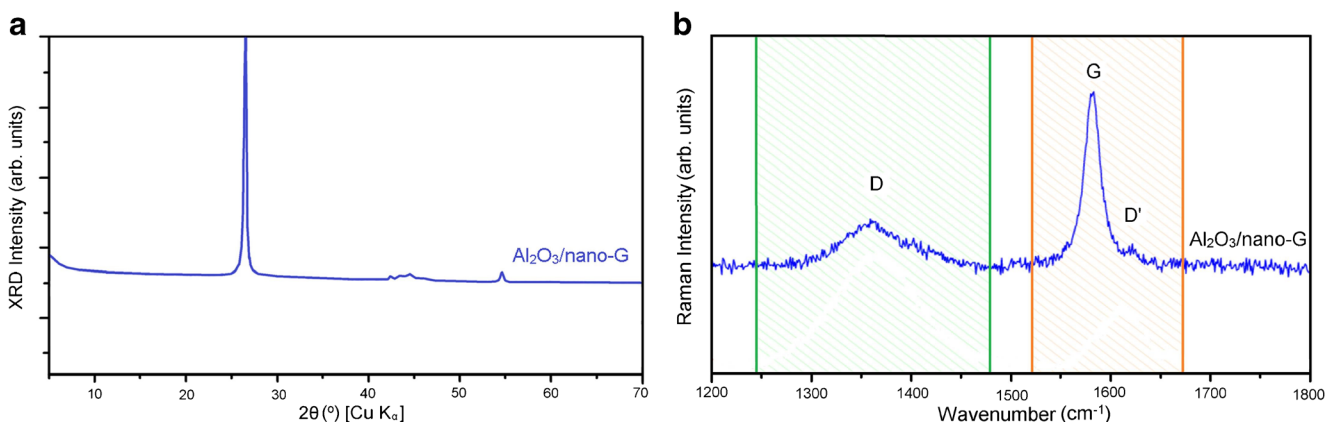
ICP-OES (Spectro Analytical Instruments GmbH, Kleve, Germany) measurements were performed using a SpectroBlue FMS16 spectrometer with inductively coupled plasma (ICP) excitation (Spectro Analytical Instruments) and a charge-coupled-device detector. The following operation parameters were used for measurements: plasma power—1.45 kW; coolant gas—Ar, 12 L min⁻¹; auxiliary gas—Ar, 1 L min⁻¹;

nebulizer gas—Ar, 1 L min⁻¹; nebulizer pressure—3.2 bar; nebulizer-cross-flow type; sample uptake rate—2 mL min⁻¹; wavelength—267.716 nm for Cr.

Ultrasonication bath with heating, EMAG, Emmi 20 HC model was purchased from EMAG Poland (Juszczyn, Poland); ultrasonic power, 150 W; working range of ultrasonic power, 50–100%; heating power, 200 W; working range of temperature, 20–80 °C; frequency, 45 kHz; and maximum volume, 1.4 L.
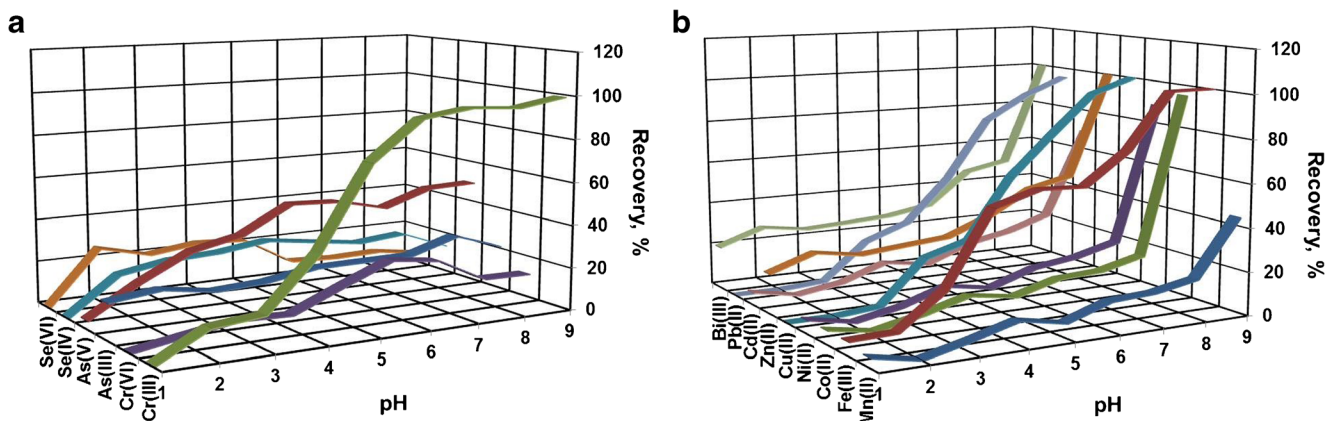
Synthesis of Al₂O₃/nano-G composite

Al₂O₃/nano-G composite was synthesized as follows: 5 g of Al(NO₃)₃ · 9H₂O, 300 mg of Triton X-100, and 1 g of high-purity graphene nanosheets were sonicated in 100 mL of water for 2 h. The black suspension was dried at 80 °C for 10 h and then heated at 500 °C for 2 h to obtained Al₂O₃ nanoparticles supported on nano-graphite (Al₂O₃/nano-G) [25].

Fig. 2 XRD patterns for Al₂O₃/nano-G (**a**) and Raman spectra obtained for Al₂O₃/nano-G (**b**)

Fig. 3 pH effect on adsorption of many metal ions including heavy-metal ions on Al_2O_3/nano-G; Cr, As, and Se (**a**); Mn, Fe, Co, Ni, Cu, Zn, Cd, Pb, and Bi (**b**) (working conditions: 1 mg of Al_2O_3/nano-G; $V = 25$ mL; $T = 25$ °C; $C_{analyte} = 250$ ng mL^{-1}; $t = 90$ min; finally technique ICP-OES)

Preparation of Al_2O_3/nano-G suspension

Two hundred fifty milligrams of Al_2O_3/nano-G was placed in 50-mL flasks and filled with high-purity water up to the mark. Directly before using, the suspension of the nanocomposite was placed in an ultrasonic bath for 30 min in order to homogenize the dispersion.
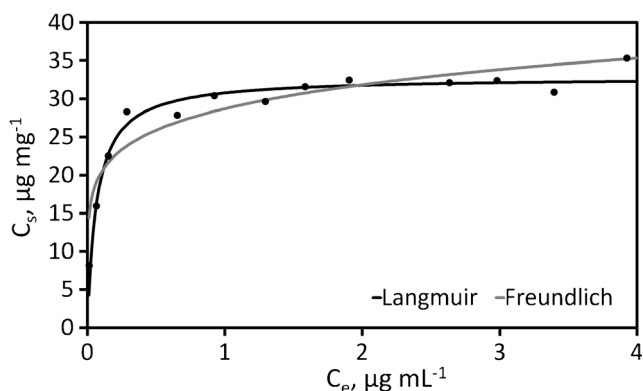
Preconcentration procedure

Two hundred-microliter aliquot of the suspension of Al_2O_3/nano-G (1 mg) was added into 25 mL of water sample. Then, the 0.1 mol L^{-1} HNO$_3$ and 0.1 mol L^{-1} NH$_3$aq were used to adjust the pH of the samples. Then, the sample was stirred for 5 min and passed through membrane filter in 2 min using the filtration assembly of 5-mm diameter. After drying for 5 min, the sample was measured by EDXRF.

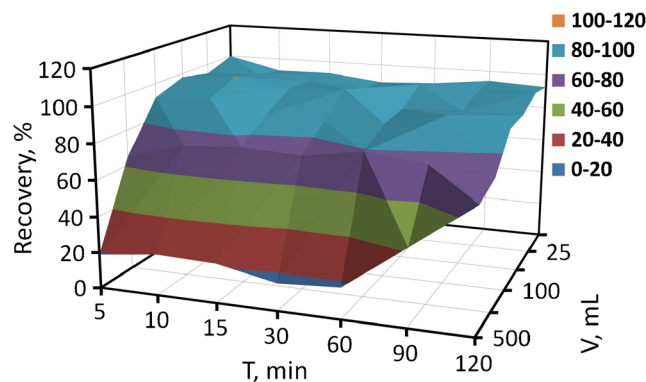The total time of sample preparation did not exceed 15 min. But using a multi-position magnetic stirrer and

two vacuum filtration kits, a series of 10 samples in 30 min can be simultaneously prepared.
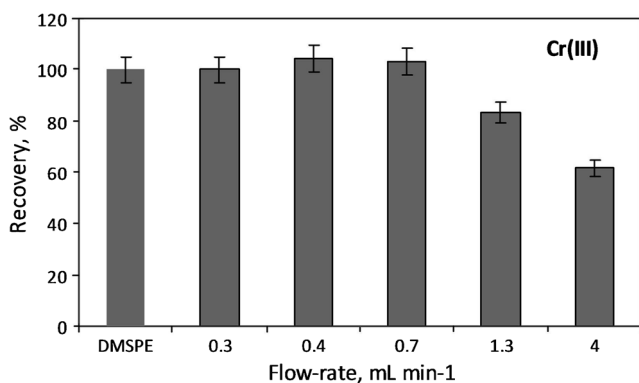
Batch adsorption

The batch adsorption experiments were carried out with 1 mg of Al_2O_3/nano-G, 25 mL of Cr(III) solutions with specified concentration, and pH. The pH values of the suspensions of Al_2O_3/nano-G and Cr(III) were adjusted with HNO$_3$ and NH$_3$aq solutions. The suspensions were stirred for 90 min to achieve adsorption equilibrium. Next, the suspensions were filtrated through membrane filters. The amount of Cr(III) ions adsorbed on Al_2O_3/nano-G (mg g^{-1}) was calculated from the difference between the initial concentration C_0 (mg L^{-1}), and equilibrium concentration C_e (mg L^{-1}) determined in filtrate by the ICP-OES spectrometry: $q_{max} = (C_0 - C_e)V/m_{adsorbent}$, where V is the volume of the suspension, and $m_{adsorbent}$ is the mass of Al_2O_3/nano-G. The recovery is given as Recovery% = $100\%(C_0 - C_e)/C_0$.

Fig. 4 Langmuir and Freundlich isotherms for Al_2O_3/nano-G towards Cr(III) ions (working conditions: 1 mg of Al_2O_3/nano-G; $V = 25$ mL; $T = 25$ °C; $C_0 = 10$ ng mL^{-1}; $t = 90$ min)

Fig. 5 The effect of contact time combined with sample volume on the recovery Cr(III) (working conditions: $m_{Al_2O_3/nano-G} = 1$ mg; $C_{analyte} = 10$ ng mL^{-1}; pH = 6.5)

Fig. 6 The effect of flow-rate for Cr(III) recovery (experimental details: Al_2O_3/nano-G membrane of mass per unit area of 0.32 mg cm^2, $c_{analyte} = 40$ ng mL^{-1}, pH = 6.5, $V = 25$ mL)

Results and discussion

Structural research

The synthesized Al_2O_3/nano-G was characterized by SEM. Figure 1a shows a SEM image of Al_2O_3/nano-G composite. As can be seen, the alumina particles are shown on the surface of the thin layer of G nanosheets. The G nanosheets are semi-transparent suggesting their few-layer nature. Both the distribution maps of C, Al, and O elements (see Fig. 1b–d) in Al_2O_3/nano-G composite as well as the good correlation between distributions of aluminum and oxygen on the surface of nanocomposite confirm the presence of Al_2O_3 nanoparticles on the surface of nano-graphite.

Al_2O_3/nano-G was also characterized by XRD and Raman spectroscopy. Figure 2a presents XRD pattern of Al_2O_3/nano-G. The pattern for Al_2O_3/nano-G is characteristic of graphite; there are not any traces of crystallized Al_2O_3. The most pronounced graphite peak at $2\Theta = 26.5°$ corresponds to coherently scattering hexagonal carbon layers with a d_{002} spacing of 3.36 Å. The diffractogram does not contain discrete patterns which could expose the presence of crystalline entities, including Al_2O_3. The absence of peaks for Al_2O_3 phase is due to the amorphous texture [26]. Instead, a plain background is recorded, with high low-angle intensity decreasing at higher theta angles. It resembles simulated XRD patterns for nano-sized, single layers of carbon structures [27].

The Raman spectrum of Al_2O_3/nano-G (see Fig. 2b) is characteristic of the nano-graphite. It consists of the intense G peak, at around 1582 cm^{-1}, that originates from the E_{2g} vibrational mode of ordered in-plane sp^2 carbons, and two, broad, and much less intense D and D′ bands at 1358 and 1621 cm^{-1}, related to the disorder of edge carbons [28]. The intensity ratio I_D/I_G is a measure of the disorder [29]. In Al_2O_3/nano-G, the I_D/I_G is equal to 0.51 indicating the prominent disorder of the G nanosheets. The main source of the disorder comes from the small size of the G nanosheets, as it is indicated by the XRD and the presence of the oxygen functional groups as well as the number of areas of sp^2 carbons with an alternating pattern of single-double carbon bonds [30] that generate huge blue shift of the G band to 1613 cm^{-1}. The absence of peaks related to Al_2O_3 confirms its amorphous structure.

pH effect

The effect of pH of aqueous solutions was investigated between 1.0 and 9.0 for a wide range of metal ions including

Table 1 Effect of coexisting ions and HA on adsorption process using Al_2O_3/nano-G as a sorbent in DMSPE/EDXRF procedure (experiment conditions: 1 mg of Al_2O_3/nano-G, 25 mL of sample volume, 10 ng mL^{-1} of Cr(III), pH = 6.5, adsorption time = 5 min)

Interferent	Concentration (μg mL^{-1})	Added as	Interferent/adsorbed ion ratio	Recovery (% ± RSD)
Na$^+$	200	NaNO$_3$	20,000	95.48 ± 0.65
K$^+$	200	KNO$_3$	20,000	105.36 ± 0.09
Mg^{2+}	200	Mg(NO$_3$)$_2$·6H$_2$O	20,000	95.61 ± 0.20
Ca^{2+}	200	Ca(NO$_3$)$_2$·4H$_2$O	20,000	94.65 ± 0.57
Fe^{3+}	10	Fe(NO$_3$)$_3$·9H$_2$O	1000	75.67 ± 0.22
	5.0		500	82.18 ± 0.82
	2.5		250	96.75 ± 0.89
NO$_3^-$	800	KNO$_3$	80,000	93.25 ± 1.14
PO$_4^{3-}$	1.0	Na$_3$PO$_4$·12H$_2$O	100	91.98 ± 1.37
SO$_4^{2-}$	300	Na$_2$SO$_4$	30,000	100.16 ± 1.57
Cl$^-$	400	NaCl	40,000	65.12 ± 1.08
	300		30,000	87.09 ± 0.42
	200		20,000	93.92 ± 0.48
HA	5.0	Humic Acid	500	80.62 ± 0.56
	4.0		400	85.07 ± 0.32
	3.0		300	94.73 ± 1.68

Table 2 The parameters characterized DMSPE/EDXRF methodology ($n = 3$)

Analyte	Analytical range (ng mL^{-1})	Equation (C, ng mL^{-1}) (I, count s^{-1})	Correlation coefficient (R)	LOD (ng mL^{-1})	LOQ (ng mL^{-1})	RMS (ng mL^{-1})	RSD (%)
Cr(III)	2.0–50	$I = 4.943C + 1.146$	0.9988	0.04	0.15	0.87	3.47

heavy metal ions. Figure 3 presents relationship between adsorption percentage of multivalent ions, such as Cr(III), Cr(VI), As(III), As(V), Se(IV), and Se(VI) (Fig. 3a) as well as mainly divalent ions, such as Mn (II), Ni(II), Cd(II), Pb(II), Co(II), Cu(II), and Zn(II) and also trivalent ions: Fe(III), Bi(III) (Fig. 3b), and solution pH. As can be seen, Al$_2$O$_3$/nano-G shows selective and high affinity for Cr(III) ions. In the acid solution up to pH 3.0, the adsorption percentage is near 20%. Between pH 4.0 and pH 6.5, the adsorption percentage increases and, at pH 6.5, Al$_2$O$_3$/nano-G achieved the maximum adsorption (95%). Above pH 6.5 and in the basic solution, adsorption percentage of Cr(III) remains at the high level. In the case of Cr(VI) ions, Al$_2$O$_3$/nano-G shows the maximum adsorption percentage (25%) in the range of pH 6.0–7.0. At pH < 6.0 and pH > 7.0, Cr(VI) ions are poorly adsorbed by Al$_2$O$_3$/nano-G with adsorption percentage below 20%. The following Cr(III) species in aqueous solution predominate: Cr^{3+} (pH $\leq$ 5.0), Cr(OH)$_2^+$ and CrOH^{2+} (pH $\cong$ 4.0–6.5), and Cr(OH)$_3$ (pH > 7.0).

Other metal ions such as As(III), As(V), Se(IV), Se(VI), Mn(II), Fe(III), Ni(II), Cu(II), Zn(II), Cd(II), Pb(II), and Bi(III) are not quantitatively adsorbed by Al$_2$O$_3$/nano-G from the solution of pH < 8. Pb(II), Cu(II), and Fe(III) are adsorbed with satisfactory results (near 100%), but only in strong basic solution (pH $\geq$ 8). The adsorption percentages of Pb(II), Cu(II), and Fe(III) at pH 6 were ca. 55%, 55%, and 70%, respectively. The adsorption percentage for As(V) being about 40% in the range of pH 4.0–6.0 is not enough to preconcentration of trace amounts of these ions. On the other hand, sorption study at pH 9.0, where the adsorption percentage was the highest for Fe(III), Co(II), Ni(II), Cu(II), Zn(II), Cd(II), Pb(II), and Bi(III), cannot be recommended due to the precipitation of metal as, e.g., hydroxides. Finally, taking into consideration both the high adsorption of metal ions and the prevention of the precipitation of metal hydroxides, the

subsequent experiments and analysis of a real sample were performed only for Cr(III) at a pH of 6.5.

Adsorption capacity

The adsorption capacity of Al$_2$O$_3$/nano-G for Cr(III) ions was investigated using Langmuir [31, 32] and Freundlich [33] isotherms. Langmuir isotherm is described by q_{max}—the maximum amount of metal ions adsorbed per unit weight of sorbent (Al$_2$O$_3$/nano-G) achieving at the high equilibrium ion concentration (mg g^{-1})—and K_L—the constant related to the free energy of adsorption (L g^{-1}). Freundlich isotherm is described by K_F and n, Freundlich constant related to the adsorption capacity (mg^{1-n} L^n g^{-1}), and the adsorption intensity, respectively.

$$q_e = \frac{q_{max} K_L C_e}{1 + K_L C_e}$$

$$q_e = K_F C_e^{1/n}$$

Isotherm parameters were obtained by fitting the adsorption equilibrium data to the isotherm models. The following results for Langmuir and Freundlich isotherms are obtained: $q_{max} = 32.8$ mg g^{-1}, $K_L = 14.9$ L g^{-1}, $R = 0.9339$, $K_F = 28.7$ mg^{1-n} L^n g^{-1}, $n = 6.68$, $R = 0.9123$. Because the adsorption isotherms are fitted better by the Langmuir model than by the Freundlich model, a chemical adsorption process is suggested. Langmuir and Freundlich isotherms are presented in Fig. 4.

Effect of contact time and sample volume

The effect of contact time combined with sample volume on the adsorption recovery of Cr(III) ions on Al$_2$O$_3$/nano-G was studied in the range of 5–120 min and 10–500 mL, respectively. The obtained results are presented in Fig. 5. In the range sample volume from 10 to 100 mL, Cr(III) ions were adsorbed with recovery above 90% in the whole studied range of time (5–120 min). For the samples of 250 mL and 500 mL, the recoveries went down step by step. For a sample of 250 mL volume, recoveries decreased from 75 to 65% depending on the sorption time for 120 min and 5 min, respectively. For 500 mL of sample volume, the average recovery for time 5–60 min was ca. 20%, but when the time of sorption was 90 min and 120 min, the recoveries increased to 40% and near 70%, respectively. Consequently, DMSPE with Al$_2$O$_3$/nano-G as a

Table 3 Determination Cr(III) and Cr(VI) in spiked high-purity water

Added (ng mL^{-1})		Obtained (ng mL^{-1})		Recovery (%)	
Cr(III)	Cr(VI)	Cr(III)	Cr(VI)	Cr(III)	Cr(VI)
0	0	< LOD	< LOD	–	–
10	0	9.22 ± 0.68	< LOD	92.2	–
0	10	< LOD	9.51 ± 0.14	–	95.1
10	10	9.65 ± 1.12	9.38 ± 0.90	96.5	93.8

Table 4 Determination of Cr(III) in spiked water samples (pH = 6.5, sample volume 25 mL, 1 mg of Al$_2$O$_3$/nano-G, 5 min of contact time); n = 3; uncertainties correspond to one standard deviation

Sample	Added (ng mL^{-1})	Cr(III) Obtained (ng mL^{-1})	Cr(III) Recovery (%)
High-purity water	0	< LOD	–
	7.5	6.94 ± 0.04	92.5
	15	13.73 ± 0.73	91.5
Mineral water[a]	0	< LOD	–
	7.5	7.93 ± 0.51	105.7
	15	16.01 ± 1.49	106.7
Mineral water[b]	0	< LOD	–
	7.5	7.68 ± 1.00	102.4
	15	15.86 ± 0.93	105.7
Tap water	0	1.25 ± 0.54	–
	7.5	8.33 ± 1.09	94.4
	15	17.3 ± 1.31	107.0

[a] Matrix, 5.00 mg L^{-1} (Na$^+$); 1.35 mg L^{-1} (K$^+$); 46.09 mg L^{-1} (Ca^{2+}); 8.51 mg L^{-1} (Mg^{2+}); 0.25 mg L^{-1} (F$^-$); 5.30 mg L^{-1} (Cl$^-$); and 172.68 mg L^{-1} (HCO$_3^-$). [b] Matrix, 9.65 mg L^{-1} (Na$^+$); 41.69 mg L^{-1} (Ca^{2+}); 5.62 mg L^{-1} (Mg^{2+}); 0.07 mg L^{-1} (F$^-$); and 131.06 mg L^{-1} (HCO$_3^-$)

sorbent can be recommended for the samples of volume ≤ 100 mL allowing to perform the sorption within only 5 min.

The Al$_2$O$_3$/nano-G composite is characterized by a large surface area and excellent dispersibility in water. Thus, it guarantees very good contact the nanocomposite with analyzed solution and in consequence the adsorption of ions as well as equilibrium state is achieved very fast (in less than 5 min as shown in Fig. 5). For comparison, the adsorption of Cr(III) ions under flow conditions was also investigated. For this purpose, the Al$_2$O$_3$/nano-G composite was deposited on filters via vacuum filtration, and then the analyzed solution was passed through loaded filters. The effect of flow-rate on chromium recovery is shown in Fig. 6. The results indicate that the adsorption of

Cr(III) ions reaches the maximum value of 100% when flow rate is at least 0.7 mL min^{-1}. So, it means that in order to obtain the high values of recovery, the adsorption of Cr(III) under flow conditions needs at least 35 min, i.e., five times longer than in the case of DMSPE (5 min).
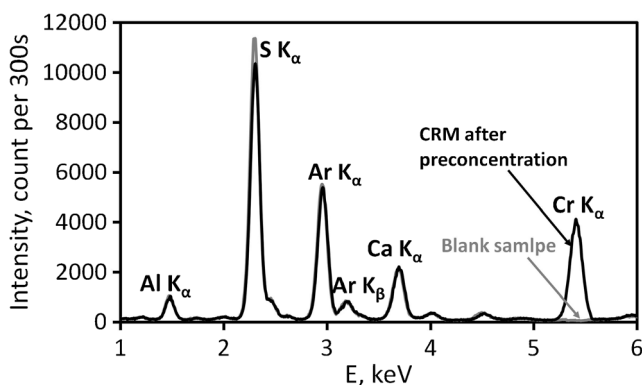
Effect of coexisting ions

The influence of coexisting ions on adsorption of Cr(III) on Al$_2$O$_3$/nano-G was investigated in the range of 20–200 μg mL^{-1} for K$^+$, Na$^+$, Ca^{2+}, and Mg^{2+}; 0.1–10 μg mL^{-1} for Fe^{3+}; 100–800 μg mL^{-1} for NO$_3^-$; 0.1–1.0 μg mL^{-1} for PO$_4^{3-}$; 100–300 μg mL^{-1} for SO$_4^{2-}$; 50–400 μg mL^{-1} for Cl$^-$; and 0.5–5.0 μg mL^{-1} for humic acid (HA). The results of these investigations are included in Table 1. The maximum studied concentration of Na$^+$, K$^+$, Mg^{2+}, Ca^{2+}, NO$_3^-$, PO$_4^{3-}$, and SO$_4^{2-}$ ions did not negatively affect the adsorption process of Cr(III) onto Al$_2$O$_3$/nano-G. According to WHO [34, 35] and EPA [36] regulations, the maximum concentrations of NO$_3^-$, SO$_4^{2-}$, and Cl$^-$ in surface waters are in the range 0–18 μg mL^{-1}, 0–250 μg mL^{-1}, and 40–63 μg mL^{-1}, respectively. Tolerance limit of Al$_2$O$_3$/nano-G in preconcentration of Cr(III) ions towards abovementioned ions are 45, 1.2, and 3.2 times better. In the groundwater, the concentrations of Mg^{2+}, Ca^{2+} [37], Fe^{3+}, NO$_3^-$ [36], SO$_4^{2-}$ [38], PO$_4^{3-}$, and Cl$^-$ [36] are not higher than 100, 100, 2.0, 50, 230, 0.7, and 250 μg mL^{-1}, respectively. Thus, as obtained results show, nanocomposite can be also used in the analysis of groundwater. Cr(III) ions can be also successfully preconcentrated on Al$_2$O$_3$/nano-G using DMSPE when the concentrations of Fe^{3+} and HA are 2.5 μg mL^{-1} and 3.0 μg mL^{-1}, respectively. Concentrations of iron in drinking water are normally less than 0.3 μg mL^{-1}. Big tolerance of the proposed method towards coexisting ions allows applying Al$_2$O$_3$/nano-G as a sorbent to determination of chromium in different kinds of water such as ca. drinking and surface water as well as groundwater.

Table 5 Determination of chromium ions in CRM (results are expressed as mean values ± standard deviations, n = 3)

Water	Mayor element of matrix (mg L^{-1})	Major trace element of matrix (μg L^{-1})	Analyte	Certified concentration (μg L^{-1})	Determined concentration (μg L^{-1})	Error (%)
NIST 1640a	Ca (5.615 ± 0.021), Mg (1.0586 ± 0.0041), K (0.5799 ± 0.0023), Si (5.210 ± 0.021), Na (3.137 ± 0.031)	Al (53.0 ± 1.8), As (8.075 ± 0.070), Ba (151.80 ± 0.83), B (303.1 ± 3.1), Cr(40.54 ± 0.30), Co (20.24 ± 0.24), Cu(85.75 ± 0.51), Fe (36.8 ± 1.8), Mn(40.39 ± 0.36), Mo (45.60 ± 0.61), Ni(25.32 ± 0.14), Pb (12.101 ± 0.050), Se(20.13 ± 0.17), Sr (126.03 ± 0.27), U(25.35 ± 0.27), V (15.05 ± 0.25), Zn(55.64 ± 0.35)	Cr	40.54 ± 0.30	39.38 ± 0.39	2.85

Fig. 7 The EDXRF spectra for blank sample (gray line) and sample after reduction using H_2SO_4/C_2H_5OH and preconcentration of Cr ions (black line) in CRM on Al_2O_3/nano-G (measurement conditions: 20 kV, 450 µA, filter: Al-200, air)

Analytical performance

The calibration curve was prepared under optimized conditions based on series of standard solutions including various concentrations of Cr(III) from 2.0 to 50 ng mL^{-1}. The characteristic of the method is presented in Table 2. Limit of detection (LOD) was calculated using the formula LOD = $(3/k)(B/t)^{1/2}$, where k is the sensitivity read from equation (mg mL^{-1} s^{-1}), B is the background count rate (counts s^{-1}), and t is the counting time (300 s). Limit of quantification (LOQ) was calculated from LOQ = 3.3· LOD. The root mean square (RMS) describes the sum of the differences between the values of the standard and

calculated concentrations. The method precision was characterized by average relative standard deviation (RSD).

The proposed method can be applied to the simultaneous determination of Cr(III), Cr(VI), and total Cr. The recoveries were examined by spiking water samples with various Cr species. In order to determine total Cr in spiked water samples (see Table 3), the prereduction step using concentrated H_2SO_4 and ethanol was applied before using the developed methodology. Cr(III) was determined directly using the developed procedure. But the concentration of Cr(VI) was calculated by subtracting the concentration of Cr(III) from total chromium concentration. The results presented in Table 3 show that various species of chromium can be successfully determined in water samples by DMSPE/EDXRF with Al_2O_3/nano-G as a sorbent.

The developed method was also successfully applied for the determination of trace amounts of chromium ions in different types of drinking water samples, e.g., mineral and tap water. Analyzed water samples were spiked with 7.5 ng mL^{-1} and 15 ng mL^{-1} of Cr(III) ions. Table 4 presents the obtained results showing that the recoveries of enriched chromium (91–107%) are reasonable for trace analysis.

Analytical application of Al_2O_3/nano-G

The obtained Al_2O_3/nano-G composite combined with the developed DMSPE/EDXRF methodology was applied to analysis of certified reference material (CRM) of natural water

Table 6 Comparison of the developed DMSPE/EDXRF methodology with the other recently published procedures based on solid-phase extraction and its miniaturized derivatives

Procedure	Sorbent	Analyte	Mass of sorbent (mg)	pH	Analytical range (ng mL^{-1})	Final technique	LOD (ng mL^{-1})	RSD (%)	Ref.
MMHSPE[a]	Fe_3O_4/Al_2O_3 NPs	Cr(III)	30	8.0	10–1000	FAAS	1.40	3.4	[40]
MSPE[b]	$Fe_3O_4@ZrO_2$ NPs	Cr(III)	50	8.0	4.0–400	FAAS	0.69	2.1	[41]
SPE-FI[c]	$Nb_2O_5–SiO_2$	Cr(III)	100	8.0	1.2–120	FAAS	0.34	4.6	[42]
MSPE	$Fe_3O_4@SiO_2@CTS$[f] magnetic NPs	Cr(III) Cr$_{total}$	20	9.0 6.0	0.1–100	ICP-OES	0.02 0.03	4.8 5.6	[39]
SPE	Oxidized SWCNTs	Cr(III) Cr(VI)	20	3.0	0.1–100	ICP-MS	0.01 0.02	2.1 4.0	[43]
SPE	Oxidized MWCNTs	Cr(III)	2.0	4.0	5.0–200	FAAS	1.15	1.7	[14]
DMSPE	Aliquat 336[j]-MWCNTs	Cr(VI)	5.0	2.0 7.5	10–3000 10–500	TXRF	3.00 2.00	11.9 9.5	[16]
DMSPE	GO	Cr(III)	0.5	6.0	1.0–150	EDXRF	0.06	1.7	[11]
Dispersive magnetic SPE	mf-GO	Cr(III) Cr(VI)	50	8.0 2.0	5.0–100	FAAS	1.60 1.40	3.4 3.0	[17]
SPE	G	Cr(III)	30	8.0	10–1000	FAAS	0.50	4.3	[18]
DMSPE	Al_2O_3/GO	Cr(III)	1.0	6.0	2.0–50	EDXRF	0.11	4.0	[24]
DMSPE	Al_2O_3/nano-G	Cr(III)	1.0	6.5	2.0–50	EDXRF	0.04	3.5	This work

[a] *MMHSPE*, magnetic mixed hemimicelles solid-phase extraction; [b] *MSPE*, magnetic solid-phase extraction; [c] *FI*, flow injection system; [f] *CTS*, chitosan; [j] *Aliquat 336*, the anionic exchanger tricaprylmethylammonium chloride

NIST 1640a. The results are shown in Table 5. As can be seen, the accuracy of the method is very good, and the calculated error was below 3%. EDXRF spectra (see Fig. 7) confirmed good peak/background ratio for chromium after its preconcentration on Al_2O_3/nano-G, which results from the excellent sensitivity of the proposed methodology.

Comparison of DMSPE/EDXRF using Al_2O_3/nano-G with other methods based on solid-phase extraction

In Table 6, recently published methodologies used for determination of trace amount of chromium ions were compared with the developed methodology. As can be noticed, the different solid-phase extraction procedures and its miniaturized derivatives play an important role in the preconcentration of trace and ultratrace amount of chromium. The advantage of the developed methodology is a fact that only 1 mg of Al_2O_3/nano-G is enough to preconcentrate trace amount of chromium ions. Meanwhile, according to Table 6, the method using $Fe_3O_4@SiO_2@CTS$ magnetic nanoparticles [39], Fe_3O_4/Al_2O_3 [40], $Fe_3O_4@ZrO_2$ [41], and Nb_2O_5–SiO_2 [42] required 20, 30, 50, and 100 times higher mass of sorbent than synthesized Al_2O_3/nano-G. Furthermore, the mass of Al_2O_3/nano-G is less than the mass of the most other carbon sorbents based on modified CNTs and GO. Obtained LOD (0.04 ng mL^{-1}) using the developed method and EDXRF as a measurement technique is better than LOD obtained using FAAS (in the range 0.34–1.60 ng mL^{-1}) [17, 42] and TXRF (3.00 and 2.00 ng mL^{-1} for aqueous samples) [16]. Al_2O_3/nano-G combined with DMSPE/EDXRF methodology allowed achieving similar LOD (0.04 ng mL^{-1}) to $Fe_3O_4@SiO_2@CTS$ magnetic nanoparticles connected with MSPE/ICP-OES (0.02–0.03 ng mL^{-1}) [39], oxidized SWCNTs combined with SPE/ICP-MS (0.01–0.02 ng mL^{-1}) [43], and GO with DMSPE/EDXRF (0.06 ng mL^{-1}) [11]. Preconcentration of chromium on Al_2O_3/nano-G allowed us to decrease the LOD of this element three times in relation to Al_2O_3/GO nanocomposite used as a sorbent [24].

Conclusion

This paper described a composite based on nano-graphite (G) covered by aluminum oxide (Al_2O_3) in selective sorption and determination of trace chromium ions in water samples using DMSPE. Al_2O_3/nano-G combined with the developed methodology played also an important role in speciation of chromium. Thanks to the combination of DMSPE with non-destructive EDXRF as a measurement technique, the chromium ions were determined fast, simple, and effectively in water samples. The advantage of DMSPE/EDXRF methodology is that the elution of analyte is not needed and the Al_2O_3/nano-G with adsorbed Cr(III) can be analyzed directly. Thus, the developed

methodology is eco-friendly and in agreement with the principles of green analytical chemistry. Compared to Al_2O_3/GO nanocomposite, Al_2O_3/nano-G is characterized by a much better limit of detection. The LOD achieved by the developed DMSPE/EDXRF procedure (0.04 ng mL^{-1}) is below the highest licit concentration of chromium ions in drinking water according to EPA regulations (100 ng mL^{-1} of total chromium) [4]. Thus, the method can be recommended to determine chromium ions in water. The accuracy of method (expressed as an error) using certificate material reference NIST 1640a was 3%. The developed method allows determining the trace amount of chromium ions in environmental water samples without unnecessary laboratory work extending time of the analytical procedure and generating additional error sources.

Compliance with ethical standards

Conflict of interest The authors declare that they have no conflict of interest.

References

1. Kotas J, Stasicka Z. Chromium occurrence in the environment and methods of its speciation. Environ Pollut. 2000;107:263–83.
2. Beyersmann D. Effects of carcinogenic metals on gene expression. Toxicol Lett. 2002;127:63–8.
3. WHO. Water Sanitation Hygiene. Chemical hazard in drinking-water: chromium. In: Background document for development of WHO Guidelines for Drinking-water Quality. 2018 http://www.who.int/water_sanitation_health/water-quality/guidelines/chemicals/chromium/en/ of subordinate document. Accessed 2018.
4. U.S. EPA. Chromium in drinking water. 2017. http://www.epa.gov/dwstandardsregulations/chromium-drinking-water of subordinate document. Accessed 24 April 2017.
5. Tunçeli A, Türker AR. Speciation of Cr(III) and Cr(VI) in water after preconcentration of its 1,5-diphenylcarbazone complex on amberlite XAD-16 resin and determination by FAAS. Talanta. 2002;57:1199–204.
6. Peng H, Zhang N, He M, Chen B, Hu B. Simultaneous speciation analysis of inorganic arsenic, chromium and selenium in environmental waters by 3-(2-aminoethylamino) propyltrimethoxysilane modified multi-wall carbon nanotubes packed micro column solid phase extraction and ICP-MS. Talanta. 2015;131:266–72.
7. Saygi KO, Tuzen M, Soylak M, Elci L. Chromium speciation by solid phase extraction on Dowex M 4195 chelating resin and determination by atomic absorption spectrometry. J Hazard Mater. 2008;153:1009–14.
8. Tuzen M, Soylak M. Multiwalled carbon nanotubes for speciation of chromium in environmental samples. J Hazard Mater. 2007;147:219–25.

9. Narin I, Kars A, Soylak M. A novel solid phase extraction procedure on Amberlite XAD-1180 for speciation of Cr(III), Cr(VI) and total chromium in environmental and pharmaceutical samples. J Hazard Mater. 2008;150:453–8.

10. Buluta VN, Ozdesa D, Bekircana O, Gundogdua A, Durana C, Soylak M. Carrier element-free coprecipitation (CEFC) method for the separation, preconcentration and speciation of chromium using an is a tin derivative. Anal Chim Acta. 2009;632:35–41.

11. Pytlakowska K. Speciation of inorganic chromium in water samples by energy dispersive X-ray fluorescence spectrometry. J Anal Atom Spectrom. 2016;31:968–74.

12. Zhang X-X, Tang S-S, Chen M-L, Wang J-H. Iron phosphate as a novel sorbent for selective adsorption of chromium(III) and chromium speciation with detection by ETAAS. J Anal Atom Spectrom. 2012;27:466–72.

13. Saxena R, Tiwari S, Sharma N. Flow-injection solid phase extraction using Dowex Optipore L493 loaded with dithizone for preconcentration of chromium species from industrial waters and determination by FAAS. RSC Adv. 2015;5:69196–204.

14. Yu H, Sun W, Zhu X, Zhu X, Wei J. Study on multi-walled carbon nanotubes on-line separation/preconcentration of chromium(III) and chromium speciation. Anal Sci. 2012;28:1219–24.

15. Gil RA, Cerutti S, Gásquez JA, Olsina RA, Martinez LD. Preconcentration and speciation of chromium in drinking water samples by coupling of on-line sorption on activated carbon to ETAAS determination. Talanta. 2006;68:1065–70.

16. Bahadir Z, Bulut VN, Hidalgo M, Soylak M, Marguí E. Determination of trace amounts of hexavalent chromium in drinking waters by dispersive microsolid-phase extraction using modified multiwalled carbon nanotubes combined with total reflection X-ray fluorescence spectrometry. Specrochim Acta B. 2015;107:170–7.

17. Islam A, Ahmad H, Zaidi N, Kumar S. A graphene oxide decorated with triethylenetetramine-modified magnetite for separation of chromium species prior to their sequential speciation and determination via FAAS. Microchim Acta. 2016;183:289–96.

18. Chang Q, Song S, Wang Y, Li J, Ma J. Application of graphene as a sorbent for preconcentration and determination of trace amounts of chromium(III) in water samples by flame atomic absorption spectrometry. Anal Methods. 2012;4:1110–6.

19. Zawisza B, Skorek R, Stankiewicz G, Sitko R. Carbon nanotubes as a solid sorbent for the preconcentration of Cr, Mn, Fe, Co, Ni, Cu, Zn and Pb prior to wavelength-dispersive X-ray fluorescence spectrometry. Talanta. 2012;99:918–23.

20. Dai B, Cao M, Fang G, Liu B, Dong X, Pan M, et al. Schiff base-chitosan grafted multiwalled carbon nanotubes as a novel solid-phase extraction adsorbent for determination of heavy metal by ICP-MS. J Hazard Mater. 2012;219– 220:103–10.

21. Wang X, Shi L, Lin Q, Zhua X, Duan Y. Simultaneous and sensitive analysis of Ag(I), Mn(II), and Cr(III) in aqueous solution by LIBS combined with dispersive solid phase microextraction using nano-graphite as an adsorbent. J Anal Atom Spectrom. 2014;29:1098–104.

22. Ghazaghia M, Mousavia HZ, Rashidib AM, Shirkhanlooc H, Rahighi R. Innovative separation and preconcentration technique of coagulating homogenous dispersive micro solid phase extraction exploiting graphene oxide nanosheets. Anal Chim Acta. 2016;902:33–42.

23. Pytlakowska K. Dispersive micro solid-phase extraction of heavy metals as their complexes with 2-(5-bromo-2-pyridylazo)-5-diethylaminophenol using graphene oxide nanoparticles. Microchim Acta. 2016;183:91–9.

24. Baranik A, Gagor A, Queralt I, Marguí E, Sitko R, Zawisza B. Determination and speciation of ultratrace arsenic and chromium species using aluminium oxide supported on graphene oxide. Talanta. 2018;185:264–74.

25. Amaisa RS, Ribeiro JS, Segatelli MG, Yoshida IVP, Luccas PO, Tarley CRT. Assessment of nanocomposite alumina supported on multi-wall carbon nanotubes as sorbent for on-line nickel preconcentration in water samples. Sep Purif Technol. 2007;58:122–8.

26. Hao J, Li Y, Liao R, Liu G, Liao Q, Tang C. Fabrication of Al$_2$O$_3$ nano-structure functional film on a cellulose insulation polymer surface and its space charge suppression effect. Polymers. 2017;9:502–20.

27. Fujimoto H. Theoretical X-ray scattering intensity of carbons with turbostratic stacking and AB stacking structures. Carbon. 2003;41: 1585–92.

28. Ferrari C, Robertson J. Interpretation of Raman spectra of disordered and amorphous carbon. Phys Rev B. 2000;61:14095–107.

29. Cançado LG, Jorio A, Martins Ferreira EH, Stavale F, Achete CA, Capaz RB, et al. Quantifying defects in graphene via Raman spectroscopy at different excitation energies. Nano Lett. 2011;11:3190–6.

30. Kudin KN, Ozbas B, Schniepp HC, Prud'homme RK, Aksay IA, Car R. Spectra of graphite oxide and functionalized graphene sheets. Nano Lett. 2008;8:36–41.

31. Langmuir I. The constitution and fundamental properties of solids and liquids. J Am Chem Soc. 1916;38:2221–95.

32. Langmuir I. The adsorption of gases on plane surfaces of glass, mica and platinum. J Am Chem Soc. 1918;40:1361–403.

33. Freundlich HMF. Uber die adsorption in lasugen. Z Phys Chem. 1916;57:385–470.

34. WHO. Nitrate and nitrite in drinking-water. In: Background document for development of WHO guidelines for drinking-water quality. 2011. http://www.who.int/water_sanitation_health/dwq/chemicals/nitratenitrite2ndadd.pdf of subordinate document. Accessed 2011.

35. WHO. Chloride in drinking-water. In: Background document for development of WHO guidelines for drinking-water quality. 2003. http://www.who.int/water_sanitation_health/dwq/chloride.pdf of subordinate document. Accessed 2003.

36. U.S. EPA. Parameters of water quality; interpretation and standards. 2001. https://www.epa.ie/pubs/advice/water/quality/Water_Quality.pdf of subordinate document. Accessed 2001.

37. WHO. Hardness in drinking-water. In: Background document for development of WHO guidelines for drinking-water quality. 2011. http://www.who.int/water_sanitation_health/dwq/chemicals/hardness.pdf of subordinate document. Accessed 2011.

38. WHO. Sulfate in drinking-water. In: Background document for development of WHO guidelines for drinking-water quality. 2004. http://www.who.int/water_sanitation_health/dwq/chemicals/sulfate.pdf of subordinate document. Accessed 2004.

39. Cui C, He M, Chen B, Hu B. Chitosan modified magnetic nanoparticles based solid phase extraction combined with ICP-OES for the speciation of Cr(III) and Cr(VI). Anal Methods. 2014;6:8577–83.

40. Tavallali H, Deilamy-Rad G, Peykarimah P. Preconcentration and speciation of Cr(III) and Cr(VI) in water and soil samples by spectrometric detection via use of nanosized alumina-coated magnetite solid phase. Environ Monit Assess. 2013;185:7723–38.

41. Wu Y-W, Zhang J, Liu J-F, Chen L, Deng Z-L, Han M-X, et al. Fe$_3$O$_4$@ZrO$_2$ nanoparticles magnetic solid phase extraction coupled with flame atomic absorption spectrometry for chromium(III) speciation in environmental and biological samples. Appl Surf Sci. 2012;258:6772–6.

42. Martendal E, Maltez HF, Carasek E. Speciation of Cr(III) and Cr(VI) in environmental samples determined by selective separation and preconcentration on silica gel chemically modified with niobium(V) oxide. J Hazard Mater. 2009;161:450–6.

43. Chen S, Zhu L, Lu D, Cheng X, Zhou X. Separation and chromium speciation by single-wall carbon nanotubes microcolumn and inductively coupled plasma mass spectrometry. Microchim Acta. 2010;169:123–8.